LETTER

https://doi.org/10.1038/s41586-018-0687-9

Twentieth-century contribution to sea-level rise from uncharted glaciers

David Parkes[1,2]* & Ben Marzeion[2]

Global-mean sea-level rise (GMSLR) during the twentieth century was primarily caused by glacier and ice-sheet mass loss, thermal expansion of ocean water and changes in terrestrial water storage[1]. Whether based on observations[2] or results of climate models[3,4], however, the sum of estimates of each of these contributions tends to fall short of the observed GMSLR. Current estimates of the glacier contribution to GMSLR rely on the analysis of glacier inventory data, which are known to undersample the smallest glacier size classes[5,6]. Here we show that from 1901 to 2015, missing and disappeared glaciers produced a sea-level equivalent (SLE) of approximately 16.7 to 48.0 millimetres. Missing glaciers are those small glaciers that we expect to exist today, owing to regional analyses and theoretical scaling relationships, but that are not represented in the inventories. These glaciers contributed approximately 12.3 to 42.7 millimetres to the historical SLE. Additionally, disappeared glaciers (those that existed in 1901 but had melted away by 2015, and that therefore cannot be included in modern global glacier inventories) made an estimated contribution of between 4.4 and 5.3 millimetres. Failure to consider these uncharted glaciers may be an important cause of difficulties in closing the GMSLR budget during the twentieth century: their contribution is on average between 0.17 and 0.53 millimetres of SLE per year, compared to a budget discrepancy of about 0.5 millimetres of GMSLR per year between 1901 and 1990. Although the uncharted glaciers will have a minimal role in sea-level rise in the future, and are less important after 1990, these findings imply that undiscovered physical processes are not required to close the historical sea-level budget.

Mass loss from glaciers forms a major component of GMSLR during the twentieth century[1]. Direct historical records of glacier mass changes are small in number compared to the total number of glaciers globally[7,8], so methods for upscaling these observations to the global scale are necessary for assessing the GMSLR budget[2–4]. The available methods cover a wide range of complexity, from geographically weighted interpolation[8], to scaling from glacier length change observations[9,10], to numerical modelling of each individual glacier based on climate observations[11]. All these methods rely on comprehensive global inventories of glaciers, which are a relatively recent development made possible by large-scale aerial mapping[12] and satellite-based Earth observation techniques[6]. Glacier inventories are therefore only reasonably representative of current or recent glacier states, with not enough information available to determine historical states. Accuracy in reconstructed SLE mass change contribution from glaciers is limited by the effective 'resolution' of the glacier inventory (the minimal glacier size the inventory can faithfully represent), which underpins the reconstructive method. Accuracy is further limited by the possibility that glaciers that have already completely disappeared contributed to mass change in the past. There is strong evidence that small glaciers are also under-represented in the most up-to-date inventories, compared to expected glacier distributions[5,6,13]. In some regions, glaciers sized below a certain threshold are deliberately excluded from the inventories[14]. Improvements in remote observation techniques alone are not an efficient way to reduce the limitation that glacier inventory resolution places on global glacier reconstructions: new and improved datasets are expensive, time-consuming to collect (requiring lots of manual labour)[15], and limited by available sensing technologies and the missions that use them. Furthermore, reducing the error in global or regional total glacier mass by an order of magnitude could require improving the effective resolution of glacier inventories by almost four orders of magnitude[5], which would necessitate a huge advance in remote sensing. It is important to note that any error in the present-day representation of small glaciers results in proportionally larger errors in reconstructions of these glaciers' change during the past, because small glaciers tend to have experienced much greater proportional changes in volume and area since pre-industrial times than have larger glaciers (Extended Data Fig. 1b). Methods to account for the limitations of glacier inventories without explicitly collecting the missing data are therefore of great interest for improving global glacier mass-change estimates, and as we suggest here, for closing the GMSLR budget.

First, we define two new classes of glaciers that need to be considered when estimating the glaciers' SLE mass change. 'Missing' glaciers are those that we expect to exist in 2015, but which are not contained in the Randolph Glacier Inventory (RGI) version 5 (RGIv5[16], the 2015 release of the RGI, with data for over 200,000 glaciers): this under-sampling is due to limitations in remote sensing methods. 'Disappeared' glaciers are those that we expect to have existed in 1901, but that melted entirely away between 1901 and 2015: they are a contribution systematically left out by glacier reconstructions that rely explicitly on modern inventories, regardless of the quality of remote sensing data. We use the term 'uncharted' glaciers to refer to the combination of these two classes of glacier.

We then combine glacier modelling and empirically determined global power laws relating glacier frequency density and glacier surface area S to estimate the 1901–2015 SLE mass loss contribution for missing and disappeared glaciers. The existence of a power-law relationship between glacier surface area and frequency density is supported by theoretical evidence[13] and observational evidence on a regional scale[5], as well as evidence of a similar power law holding for smaller snow-deposition-based phenomena such as snow patches[13]. We find strong evidence for the same form of power law holding globally (Fig. 1). From RGIv5 data, the power law holds globally for glaciers between $10^{0.3}$ (about 2) km^2 and $10^{2.6}$ (about 398) km^2, with the fall-off in frequency density for large glaciers a consequence of the limitations in size and topography of glacierized regions. The fall-off in frequency density for small glaciers ($10^{-2.0}$ (=0.01) km$^2 \leq S < 10^{0.3}$ km^2, where the lower limit of $10^{-2.0}$ km^2 is the minimum glacier size in RGIv5), however, does not have a known physical justification. As the power law holds both for a wide range of mid-sized glaciers, and also for smaller but similarly distributed phenomena such as snow patches[5], and since there is no posited mechanism reducing the occurrence of small glaciers, the fall-off at small glacier sizes has been hypothesized to be explained by under-representation in the global inventory[5,6]. On the basis of this hypothesis, we derive an upper-bound estimate of the contribution of uncharted glaciers.

[1]Institute of Atmospheric and Cryospheric Sciences, University of Innsbruck, Innsbruck, Austria. [2]Institute of Geography, University of Bremen, Bremen, Germany.
*e-mail: david.parkes.88@gmail.com

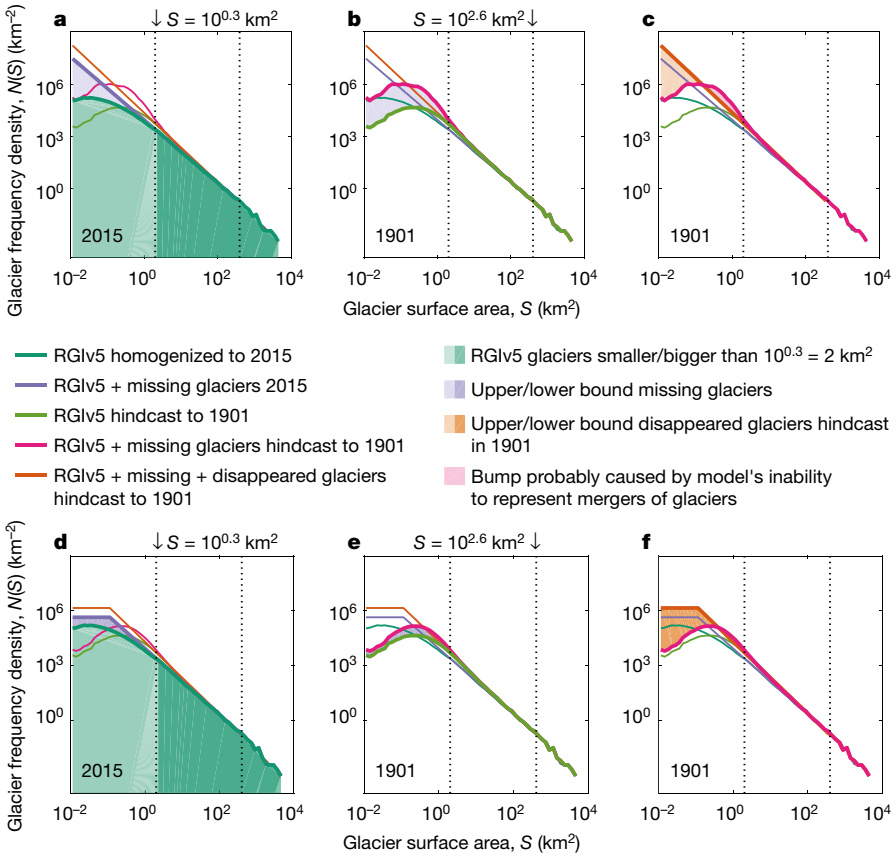

Fig. 1 | Frequency density of glaciers as a function of glacier size. The top and bottom rows show the upper and lower bounds respectively. Within each row, each panel shows the same set of distributions, but highlights different distributions, representative of a different set of glaciers. **a**, **d**, The RGIv5 glacier distribution in 2015 (split into light/dark green for small/larger glaciers) and the power-law-derived distribution of missing glaciers in 2015. **b**, **e**, The distribution of missing glaciers in 1901. **c**, **f**, The 1901 distribution of disappeared glaciers, as well as a 'bump' that we consider to be a modelling artefact.

The hypothesis that the power law holds down to the smallest glacier size classes remains to be tested, so we also derive a lower-bound estimate of the contribution of uncharted glaciers. The lower bound assumes that there is a cut-off in glacier size for which the power law holds, and that the frequency density of glaciers smaller than the cut-off, as a function of area, is constant. The chosen cut-off of 0.1 km^2 is an order of magnitude larger than the minimum glacier size recorded in RGIv5, implying that the lower-bound estimate is considerably less affected by potential effects from ice bodies at the glacier or snow-patch transition. These borderline glaciers are not necessarily dominated by the same physical processes as larger glaciers, so scaling relationships may be less certain. The upper and lower bounds account for a range of possibilities of partial flattening or tailing-off of the power law at the smallest glacier sizes. Observations in Switzerland show power-law behaviour extending down to smaller glacier sizes than in the global dataset, but with a smaller exponent (Methods and Extended Data Fig. 2). If the Swiss data are globally representative, this suggests a reality falling comfortably between the upper and lower bounds.

To account for missing glaciers, we scale up the mass change from small glacier size classes in RGIv5. For the upper bound, using the power law observed for glaciers between $10^{0.3}$ km^2 and $10^{2.6}$ km^2, we generate an upscaling factor for each glacier size class below $10^{0.3}$ km^2 equal to the ratio of the power-law-predicted 2015 frequency density to the 2015 RGIv5 frequency density. The lower bound has size classes below 0.1 km^2 scaled to the frequency density at 0.1 km^2. By hindcasting the annual mass change for each glacier in RGIv5 back to 1901 using an established global glacier model[11] that has been used extensively in sea-level budget assessment[2–4,17,18], and applying these upscaling factors to the contribution of each small glacier ('small' according to their 2015 size), we generate mass change estimates for missing glaciers between 1901 and 2015. As the 1901 glaciers are also expected to be distributed following a power law, we independently fit a power law to the RGIv5 + missing glaciers in 1901, and this time upscale the 1901 mass, using newly generated upscaling factors, to account for the total mass of disappeared glaciers. The glacier mass added by this second upscaling is expected to have entirely disappeared by 2015, so by combining the total mass of disappeared glaciers and the 1901–2015 mass change from missing glaciers, we arrive at upper- and lower-bound total mass change estimates for all uncharted glaciers during the period 1901–2015.

The RGIv5 glacier frequency distribution for 2015 (Fig. 1a, d, dark green line) gives a power-law exponent of -1.80 ± 0.01 (Fig. 1a, d, purple line), resulting in an upper/lower bound of $42.7 \pm 6.5/12.3 \pm 1.6$ mm SLE (95% confidence interval; see the 'Estimation of errors' section in the Methods for details) mass loss between 1901 and 2015 from missing glaciers. The power-law fit applied to the 1901 glacier distribution including upper-bound missing glaciers (Fig. 1b, pink line) gives an exponent of -1.98 ± 0.04 (Fig. 1c, orange line), resulting in an expected upper bound of 5.3 ± 2.4 mm SLE mass loss over the same period from disappeared glaciers. Applied to the lower 1901 glacier distribution with lower-bound missing glaciers (Fig. 1e, pink line) the power-law fit gives an exponent of -1.96 ± 0.03 (Fig. 1f, orange line), and a lower bound of 4.4 ± 1.4 mm SLE mass loss from disappeared glaciers. We note that the different exponents for 2015 and 1901 may be because of the state of glaciers relative to equilibrium, as the response of smaller glaciers is faster than the response of large glaciers, resulting in a 'flattening' of the distribution as glaciers in general shrink. Bahr and Radic[5] find a regionally averaged (across ten glacierized regions) exponent of -2.10 ± 0.09, and the theoretical exponent given by Bahr and Meier[13] is -2.05, implicitly for an equilibrium scenario. We see a

Table 1 | Breakdown of current ice mass and mass changes

	Total ice mass in 2015 (mm SLE)	Mass loss contribution 1901–2015 (mm SLE)
RGIv5 glaciers $\geq 10^{0.3}$ km^2	489.3 ± 21.4	75.1 ± 3.3
RGIv5 glaciers $< 10^{0.3}$ km^2	3.2 ± 0.1	14.0 ± 0.6
RGIv5 total	**492.5 ± 21.6**	**89.1 ± 3.9**
Missing glaciers (upper bound)	2.4 ± 0.4	42.7 ± 6.5
Disappeared glaciers (upper bound)	0	5.3 ± 2.4
Uncharted glaciers (upper bound)	**2.4 ± 0.4**	**48 ± 8.9**
Missing glaciers (lower bound)	2.1 ± 0.3	12.3 ± 1.6
Disappeared glaciers (lower bound)	0	4.4 ± 1.4
Uncharted glaciers (lower bound)	**2.1 ± 0.3**	**16.7 ± 3.0**

Current ice masses and 1901–2015 SLE mass loss contributions from different glacier subsets (95% uncertainty ranges). Boldface rows are the sum of the previous two rows. In the RGIv5 results—as in the missing glaciers—we see that a small glacier mass in 2015 was responsible for a much larger proportion of historical glacier mass loss than their 2015 mass may suggest, as these glaciers have typically seen a much greater proportionate mass change than large glaciers (see also Extended Data Fig. 1b). Disappeared glaciers, by definition, do not exist in 2015, but still contributed a modest amount to SLE mass loss.

slightly flatter distribution in 1901 and a flatter distribution still in in 2015, qualitatively in agreement with general glacier shrinkage during the twentieth century.

Combining the contributions of missing and disappeared glaciers, we derive a total mass loss upper bound of 48.0 ± 8.9 and a lower bound of 16.7 ± 3.0 mm SLE from uncharted glaciers. The revised mass change figure from the reconstruction of all RGIv5 glaciers using the unmodified glacier model[11] forced with the climate observations[19] (Climate Research Unit (CRU) version 3.24) and initialized using RGIv5[16] is 89.1 ± 3.9 mm SLE. Uncharted glaciers have therefore contributed 35.0% of a total 137.1 ± 12.8 mm SLE glacier mass loss between 1901 and 2015 (using upper bound values), and 15.8% of a total 105.8 ± 6.9 mm SLE (using lower bound values). The SLE 2015 mass and 1901–2015 mass loss contribution for each class of glacier is summarized in Table 1.

The uncharted glacier contribution to GMSLR over the period 1901–2015 is estimated to be between 0.15 and 0.42 mm of SLE per year, and the total glacier contribution during the same period to be between 0.93 and 1.20 mm of SLE per year. The upper bound uncharted contribution may close the sea-level budget discrepancy identified in the IPCC's Fifth Assessment Report[3] for 1901 to 1990 (0.17/0.53 mm of SLE per year lower/upper bound contribution compared to a discrepancy of 0.5 mm of GMSLR per year), but only covers part of the discrepancy for 1993 to 2010 (0.08/0.21 mm of SLE per year lower/upper bound contribution compared to a discrepancy of 0.4 mm of GMSLR per year). Smaller estimates of twentieth-century GMSLR have been published since the IPCC Fifth Assessment Report[20,21]. However, because their methods (to different degrees) depend on the sea-level fingerprint of glacier mass loss, the impact of our results on a sea-level budget closure based on these recent GMSLR estimates is not immediately obvious.

The modelled annual SLE mass loss contribution between 1901 and 2015 for RGIv5, missing, and disappeared glaciers is shown in Fig. 2. The data from RGIv5 glaciers is split into the contribution from small glaciers (which contributes to the upscaling of the uncharted glaciers) and that from larger glaciers. This shows that the contribution of uncharted glaciers, both in absolute terms and as a proportion of total glacier contribution, is largest early in the twentieth century. The contribution decreases gradually to the point where it is negligible by 2015, with the total remaining volume of missing glaciers in 2015 comprising only between 2.1 ± 0.3 and 2.4 ± 0.4 mm of SLE ice mass. This potential contribution is likely to be realized in the very near future, as missing glaciers are very small, and from past surface mass balances (Extended Data Fig. 1a) we can see that small glaciers tend to have more rapid proportionate mass changes. The decreasing pattern of mass loss for uncharted glaciers is largely distinct from the overall pattern of RGIv5 mass change, which shows increasing mass loss rates up to a peak in the 1930s, decreasing to a minimum around 1970, and subsequent increase until the 2010s (this temporal pattern is the result of spatially inhomogeneous climate variability during the twentieth century[11]).

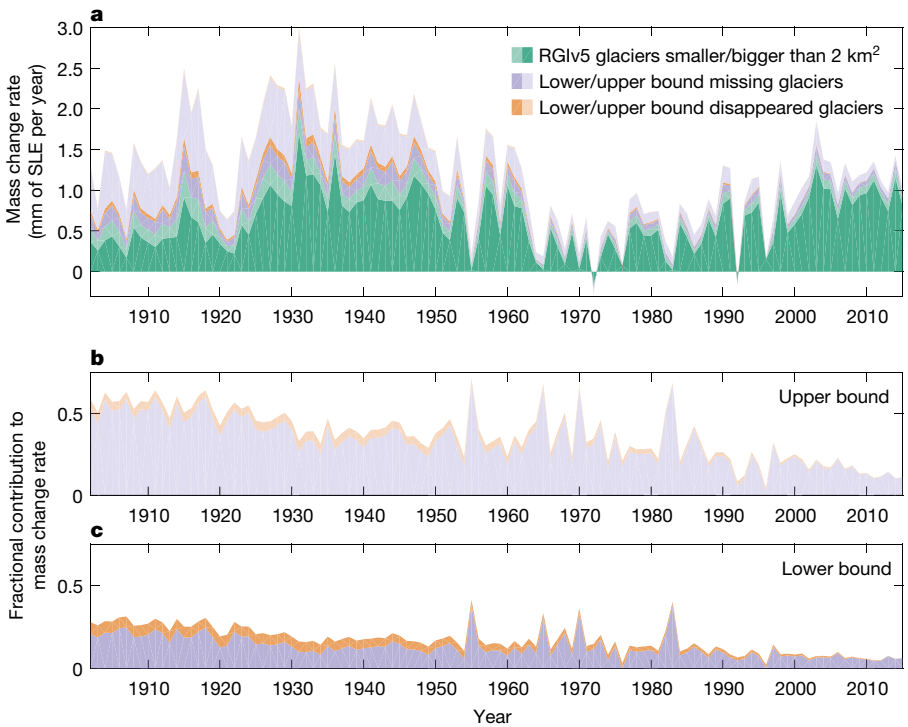

Fig. 2 | Annual glacier mass loss time series. The light and dark green sections show the hindcast mass loss from RGIv5 glaciers. The additional contribution from missing glaciers is shown in purple, and that of disappeared glaciers is shown in orange. **a**, The lower and upper bounds are stacked (light and dark purple combined give the upper bound of the missing glaciers' contribution, light and dark orange combined that of the disappeared glaciers). **b**, **c**, The missing and disappeared glaciers' upper-bound (**b**) and lower-bound (**c**) contributions, respectively, are separated, and the fractional mass changes are calculated based on the separate totals.

The consideration of uncharted glaciers adds a substantial amount to hindcast SLE mass loss contributions from glaciers between 1901 and 2015 that is comparable to the existing discrepancy between known GMSLR contributors and observed sea-level change. It is therefore imperative for the closure of the twentieth-century GMSLR budget that these glaciers are considered. Although higher-quality observational datasets can reduce the need for upscaling to account for uncharted glaciers, these are limited by the timeframes and technical development of Earth observation missions. In the case of disappeared glaciers, even a theoretically perfect inventory still cannot represent their mass changes. Accounting for uncharted glaciers thus cannot be done exclusively through improvements in glacier inventories, and upscaling (or other methods) of contributions from known glaciers to account for glaciers outside of either the resolution or scope of current glacier inventories must form an integral part of accurate GMSLR hindcasting.

Online content

Any methods, additional references, Nature Research reporting summaries, source data, statements of data availability and associated accession codes are available at https://doi.org/10.1038/s41586-018-0687-9.

Received: 1 September 2017; Accepted: 10 September 2018;
Published online 21 November 2018.

1. Church, J. et al. in *Climate Change 2013: The Physical Science Basis* (eds Stocker, T. et al.) Ch. 13 (IPCC, Cambridge Univ. Press, Cambridge/New York, 2013).
2. Gregory, J. M. et al. Twentieth-century global-mean sea-level rise: is the whole greater than the sum of the parts? *J. Clim.* **26**, 4476–4499 (2013).
3. Church, J. A., Monselesan, D., Gregory, J. M. & Marzeion, B. Evaluating the ability of process based models to project sea-level change. *Environ. Res. Lett.* **8**, 014051 (2013).
4. Slangen, A. et al. Anthropogenic forcing dominates global mean sea-level rise since 1970. *Nat. Clim. Change* **6**, 701–705 (2016).
5. Bahr, D. & Radic, V. Significant contribution to total mass from very small glaciers. *Cryosphere* **6**, 763–770 (2012).
6. Pfeffer, W. T. et al. The Randolph Glacier Inventory: a globally complete inventory of glaciers. *J. Glaciol.* **60**, 537–552 (2014).
7. Zemp, M. et al. Historically unprecedented global glacier decline in the early 21st century. *J. Glaciol.* **61**, 745–762 (2015).
8. Cogley, J. G. Geodetic and direct mass-balance measurements: comparison and joint analysis. *Ann. Glaciol.* **50**, 96–100 (2009).
9. Oerlemans, J., Dyurgerov, M. & van de Wal, R. S. W. Reconstructing the glacier contribution to sea-level rise back to 1850. *Cryosphere* **1**, 59–65 (2007).
10. Leclercq, P. W., Oerlemans, J. & Cogley, J. G. Estimating the glacier contribution to sea-level rise for the period 1800–2005. *Surv. Geophys.* **32**, 519–535 (2011).
11. Marzeion, B., Jarosch, A. H. & Hofer, M. Past and future sea-level change from the surface mass balance of glaciers. *Cryosphere* **6**, 1295–1322 (2012).
12. WGMS (World Glacier Monitoring Service) and National Snow and Ice Data Center (NSIDC). *World Glacier Inventory* http://nsidc.org/data/glacier inventory/index.html (WGMS and NSIDC, 1989).
13. Bahr, D. B. & Meier, M. F. Snow patch and glacier size distributions. *Water Resour. Res.* **36**, 495–501 (2000).
14. Rastner, P. et al. The first complete inventory of the local glaciers and ice caps on Greenland. *Cryosphere* **6**, 1483–1495 (2012).
15. Paul, F. et al. The glaciers climate change initiative: methods for creating glacier area, elevation change and velocity products. *Remote Sens. Environ.* **162**, 408–426 (2015).
16. Arendt, A. et al. *Randolph Glacier Inventory—a Dataset of Global Glacier Outlines: Version 5.0* https://www.glims.org/RGI/randolph50.html (Global Land Ice Measurements from Space, Boulder, 2015).
17. Frederikse, T. et al. Closing the sea level budget on a regional scale: trends and variability on the Northwestern European continental shelf. *Geophys. Res. Lett.* **43**, 10864–10872 (2016).
18. Marcos, M. et al. Internal variability versus anthropogenic forcing on sea level and its components. *Surv. Geophys.* **38**, 329–348 (2017).
19. Harris, I., Jones, P., Osborn, T. & Lister, D. Updated high-resolution grids of monthly climatic observations—the CRU TS3.10 dataset. *Int. J. Climatol.* **34**, 623–642 (2014).
20. Hay, C. C., Morrow, E., Kopp, R. E. & Mitrovica, J. X. Probabilistic reanalysis of twentieth-century sea-level rise. *Nature* **517**, 481–484 (2015).
21. Dangendorf, S. et al. Reassessment of 20th century global mean sea level rise. *Proc. Natl Acad. Sci. USA* **114**, 5946–5951 (2017).

Acknowledgements This research is funded by the Austrian Science Fund (FWF) project P25362.

Reviewer information *Nature* thanks W. Pfeffer and the other anonymous reviewer(s) for their contribution to the peer review of this work.

Author contributions D.P. and B.M conceived and designed the study. B.M. performed the glacier model experiments. D.P. then developed and applied the upscaling techniques and performed the analysis. D.P. wrote the manuscript with contributions by B.M.

Competing interests The authors declare no competing interests.

Additional information
Extended data is available for this paper at https://doi.org/10.1038/s41586-018-0687-9.
Supplementary information is available for this paper at https://doi.org/10.1038/s41586-018-0687-9.
Reprints and permissions information is available at http://www.nature.com/reprints.
Correspondence and requests for materials should be addressed to D.P.
Publisher's note: Springer Nature remains neutral with regard to jurisdictional claims in published maps and institutional affiliations.

METHODS

The mass balance model used for hindcasting glacier evolution is the same as that described in ref. [11], with the output updated for the RGIv5[16] and CRU 3.24 climate observations[19]. The only modification is a change to the handling of data gaps to make it consistent with the treatment of uncharted glaciers: instead of assuming regional mean rates of glacier volume and area change for glaciers, which cannot be explicitly modelled (22.7% of all glacier area globally, of which 76.8% comes from Antarctic and Subantarctic peripheral glaciers; see Extended Data Table 1 for breakdown), the regional mean rates for glaciers within the same size class (as defined below) are assumed. For Antarctic and Subantarctic peripheral glaciers, where CRU data are not available so no glaciers can be explicitly modelled, global mean rates for glaciers within the same size class are assumed. See Methods section 'Impact of Antarctic peripheral glaciers' for a detailed consideration of the validity of using Antarctic peripheral glaciers in this study. We note that all SLE mass change values assume a global sea surface area of 3.619×10^{14} m^2.

A 'base' run of the glacier model is established first. We require a snapshot of global glacier area distribution for a single point in time, but the observation years for RGIv5 glaciers differ. We model each glacier forward to 2015 if it has an observation year before 2015, to homogenize the data to a single snapshot in 2015 (distributed as shown in the dark green line in Fig. 1a, d), as well as hindcasting their sizes in 1901 (distributed as shown by the light green line in Fig. 1b, e).

The results for all glaciers are separated into size classes based on their modelled areas in 1901 and 2015. Size classes are logarithmic, defined as each set of glaciers with surface area S such that $10^{0.1i}$ km$^2 \leq S < 10^{0.1(i+1)}$ km^2 for each integer i with $-20 \leq i < 40$ (resulting in size classes that span from 0.01 km^2 to 10,000 km^2). As these size classes do not cover equal area ranges, we divide the glacier count in each size class (unitless) by the width of each size class (upper area limit minus lower area limit, in units of km^2) to get the glacier frequency density, $N(S)$, (in units of km^{-2}). It is glacier frequency that we work with for the power law.

From the distribution of glaciers in 2015, we can determine a power law of the form $N(S) = aS^b$ (with a and b coefficients to be determined) for glacier frequency density by surface area that holds for glaciers not at either extreme end of the area distribution, with the theoretical basis in ref. [13], and extending a regional method[5]. In this specific case, we fit the regression line (purple line in Fig. 1a, d) for glaciers between $10^{0.3}$ and $10^{2.6}$ km^2, with this range selected based on the section of the graph that best fits a straight line while encompassing as many size classes as possible. We note that the regression coefficient is only generated once, globally, rather than for individual regions: this is because the distribution of differently sized glacierized regions is also part of the underlying distribution, and the power-law exponent calculated globally is not necessarily the same as the mean of exponents calculated for each region. Thus, the mass of uncharted glaciers calculated globally is not necessarily the same as the sum of the masses of uncharted glaciers if they were calculated for individual regions. In the context of SLE mass loss contributions, it is important to consider the entirety of the glacierized area rather than focusing on individual regions selected based on geographical convenience.

Estimation of errors. We generate the error values on the regression coefficients by varying the size classes over which the regression is calculated. The upper and lower limits are varied by one size class in each direction, independently, and the resulting distribution of 9 regression coefficients (lower limits of 23rd, 24th and 25th size classes, upper limits of 45th, 46th and 47th size classes in each possible combination) is used as a sample for generation of a 95% confidence interval. The regression coefficient error is generated independently for each of the two regressions performed (one to account for missing glaciers, one to account for disappeared glaciers), which results in a larger proportionate error for disappeared glacier SLE mass loss contribution. The 4.4% proportionate error from the original Marzeion[11] model is assumed to hold also for missing and disappeared glaciers and thus added to the error due to the power laws, to determine the total error for these mass loss contributions.

Missing glaciers. In this Letter, 'small glaciers' is taken to mean glaciers with area $10^{-2.0}$ km$^2 < S < 10^{0.3}$ km^2, that is, glaciers below the size of those to which the power law is fitted. We determine a scaling factor for each small glacier size class equal to the ratio of the power-law-predicted frequency density in 2015 to the observed frequency density in 2015 (with a lower cut-off in glacier size for the lower-bound estimate). To obtain an estimate of the missing glacier mass change, the contribution of each RGIv5 small glacier is multiplied by the scaling factor for the 2015 size class it occupies (regardless of what size class the same glacier may have occupied historically). Missing glaciers are defined as those small glaciers that are not included in RGIv5, but are expected to exist in 2015 from this power-law upscaling. The hindcast 1901 glacier distribution with missing glacier scaling applied is shown by the pink line in Fig. 1b, e. The annual GMLSR contribution from missing glaciers is then found by applying the upscaling factors based on 2015 glacier size class to each glacier's mass-change timeseries for RGIv5 small glaciers.

Disappeared glaciers. We fit the disappeared glacier power law (orange line in Fig. 1c, f) in the same manner as the power law for missing glacier upscaling, but with the pink line (RGIv5 + missing glaciers, hindcast to 1901) as the basis for the calculation of the power-law constant and exponent. However, a correction is needed for the 'bump' in the hindcast RGIv5 + missing glaciers. In large part, we believe this 'bump' to be due to the fact that the glacier model is unable to resolve the merging of two glaciers within a larger valley if they grow (or correspondingly, recombine glaciers, when hindcasting, that were previously the same glacier but split as they shrank); modern separate glaciers in adjoining valleys may have historically been part of a single larger glacier, but the fact that in the 1901 hindcast they are always represented as two separate glaciers artificially inflates some of the smaller size classes in the RGIv5 + missing glacier 1901 distribution, while reducing the glacier count in larger size classes. For this reason, we do not apply any scaling to small glacier size classes for which the power-law-predicted disappeared glacier frequency is lower than the RGIv5 + missing 1901 glacier frequency. The impact of this omission is not expected to be large, and we expect that it results in an overall underestimation of the disappeared glacier SLE mass-loss contribution, because the artificial inflation of size classes below $10^{0.3}$ km^2 and reduction of larger size classes is expected to result in a smaller power-law exponent. The smaller the power-law exponent (that is, the 'flatter' the distribution for the size classes on which the power law is calculated), the smaller the disappeared glacier mass added through our upscaling.

The time series shown in Fig. 2 (light and dark orange) is not explicitly calculated for disappeared glaciers. Whereas missing glaciers are upscaled on the basis of existing RGIv5 glaciers, disappeared glaciers have no existing analogues for time series upscaling. It is theoretically possible to generate a time series of mass loss by recalculating the power law on a yearly basis and determining how much of the original 1901 disappeared glacier mass is remaining, but the variability in the power-law exponent is almost certain to dominate over actual climate-driven variability. As we know that the contribution is zero in 2015 owing to these glaciers being entirely melted away, we instead show a linear decrease from a maximum in 1901, which is close to what we observe in missing glaciers.

Upper- and lower-bound estimates. We refer to the scaling of all small glacier size classes up to the power laws as the upper-bound contribution estimate. To obtain the lower-bound contribution estimates, we include an additional step: instead of upscaling all small glacier size classes to the calculated power law, we impose a cap on glacier frequency density based on the frequency density at 0.1 km^2, and upscale only to this cap for size classes between 0.01 km^2 and 0.1 km^2. This modified upscaling can be seen in Fig. 1d (for missing glaciers) and Fig. 1f (for disappeared glaciers).

In Extended Data Fig. 2, we show the glacier distribution for Switzerland alone, in order to examine the apparent power law for a region where we expect the available glacier inventories to be much more complete. The Swiss Glacier Inventory[22] is based on 25-cm-resolution aerial orthophotographs, and as we see in Extended Data Fig. 2, it gives us an apparent power law of exponent 1.16 down to the smallest measured glacier sizes in the RGI. In fact, the RGI itself also exhibits such a power law—with exponent 1.26—across small glaciers, and is apparently no less complete for this region than the SGI. With the limited number of glaciers in the SGI (1,420 in total) and in the RGI restricted to Switzerland, we do not have enough data to determine a power law for larger glaciers, so we are unable to say whether this lower-exponent power law is a characteristic of the region, or a characteristic of the distribution of smaller glaciers with a transition into a steeper power law for larger glaciers. As a compromise, instead of guessing at transitions between power laws for different glacier size scales, we suggest a lower-bound estimate of the uncharted glaciers' contribution by assuming a cut-off at 0.1 km^2, so the power law observed for larger glaciers continues down to 0.1 km^2, and below this the distribution is flat. The exponent observed in Switzerland lies somewhere between the lower bound (effectively an exponent of 0) and the upper bound, with the exponent of around 1.8 derived from larger glaciers globally.

For missing glaciers, the upper- and lower-bound estimates are based on the same power law, calculated for RGIv5 glaciers homogenized to 2015, but for disappeared glaciers, because the power law is based on the distribution of RGIv5 + missing glaciers hindcast to 1901 and this differs based on the upscaling used for missing glaciers, the upper- and lower-bound estimates are based on separately calculated power laws, with different exponents. In practice, we note a slightly smaller exponent (but not by much) for the lower-bound estimate, probably owing to the lessened effect of the merging of glaciers when hindcasting caused by the model not accounting for glaciers coming together as their area increases (see 'bump' in Fig. 1c, with a much less noticeable bump in Fig. 1f). We also note that the lower-bound contribution for missing glaciers is by definition smaller than the upper bound, because the upscaling is from the same

base glacier distribution to a strictly smaller-than-pure-power-law distribution. This is not the case for the lower-bound contribution of disappeared glaciers. Owing to the potentially different power-law exponents and the different distributions that are being upscaled from, the lower-bound disappeared-glacier contribution could be larger than the upper-bound contribution, although in practice this is not the case.

Impact of Antarctic peripheral glaciers. Glaciers in the RGIv5 Antarctic and Subantarctic region are unique in this study, as our climate data does not extend to these latitudes. This means that none of the glaciers in this region can be explicitly modelled (Extended Table 1), so global mean mass balance within each size class is assumed for each glacier. This is a strong and not well justified assumption, so it is worthwhile to consider both why it is still valuable to include these glaciers in our analysis, and what the impact on the results is if the region is removed.

Inclusion of Antarctic and Subantarctic peripheral glaciers is desirable, if possible, because the basis for a global upscaling of small glaciers must be a global glacier inventory. Generation of independent power laws on a regional basis and summing the upscaling for uncharted glaciers over these regions does not yield the same results as performing the upscaling based on global glacier distribution, and the distribution of glaciers across regions containing different-sized glacier populations is fundamentally part of the global distribution we are trying to represent. Furthermore, the definition of the RGI regions is largely a matter of convenience, and the ability to artificially partition the world's glaciers into geographically separate boxes does not reflect the fact that the overall distribution of glaciers is the result of the interaction of much less separable factors such as topography, precipitation and surface energy balance, which are variables that are more continuous across glaciated and non-glaciated areas. In the same way that individual glaciers within a region are part of a larger pattern of glacierized area within that region, individual regions are part of a larger pattern of glaciated regions across the globe. Antarctic and Subantarctic peripheral glaciers are part of this global distribution, so we consider their inclusion worthwhile despite the additional modelling assumption, provided they do not have a clearly destabilizing influence on the overall results.

Although the Antarctic and Subantarctic region comprises a large amount of overall glacier mass, it does not represent a large proportion of the total area of small glaciers (4.7%, as compared to 43.1% and 19.3% in the Greenland Periphery and Central Asia regions, respectively). Small glaciers are the ones that contribute to the upscaling for uncharted glaciers, so lack of explicit surface mass balance modelling for Antarctic and Subantarctic peripheral glaciers does not have a larger effect on the upscaled glacier SLE mass-loss contribution. Nevertheless, for completeness we provide data for the global modelling and upscaling with the Antarctic and Subantarctic region removed, corresponding to the same data included in the main text including the region. Only the upper-bound estimate is compared, as the intention is to give an impression of the maximal effect of including or removing Antarctic and Subantarctic glaciers. Removing Antarctic and Subantarctic glaciers, the RGIv5 SLE mass-loss contribution is reduced to 75.8 ± 3.3 mm SLE (from 89.1 ± 3.9 mm including Antarctic and Subantarctic peripheral glaciers), but the missing- and disappeared-glacier contributions actually increase (insignificantly; $P = 0.14$ and 0.50 respectively) to 49.1 ± 5.2 mm and 6.3 ± 2.5 mm SLE respectively (from 42.7 ± 6.5 mm and 5.3 ± 2.4 mm SLE, respectively, including the Antarctic and Subantarctic peripheral glaciers). The reason for the increase in these contributions when Antarctic and Subantarctic glaciers are removed appears to be a change in power-law exponents to -1.83 ± 0.01 for the initial missing-glacier upscaling and -2.01 ± 0.04 for the disappeared-glacier upscaling (from -1.80 ± 0.01 and -1.98 ± 0.04 respectively); these increase the amount of upscaling applied for small glacier size classes by enough to more than account for the reduced overall number of RGIv5 small glaciers used in the dataset, given the aforementioned small proportion of small glaciers that are found in the Antarctic and Subantarctic region.

Exponent constraints. The nature of the power-law explanation of glacier distribution places certain constraints on the power law in order for the outcome to be physically plausible. We concern ourselves with three integrals that relate to the distribution:

$$\int_m^n N(S)\,\mathrm{d}S \tag{1}$$

giving the total number of glaciers with area between m and n

$$\int_m^n SN(S)\,\mathrm{d}S \tag{2}$$

giving the total area of all glaciers with areas between m and n, and

$$\int_m^n jS^k N(S)\,\mathrm{d}S \tag{3}$$

giving the total volume of all glaciers with areas between m and n, with the exponent k and constant j being volume/area scaling factors $k = 1.375$ and $j = (0.0340\ \mathrm{km})^{(3-2k)}$ taken from literature[23,24]. In our analysis, we find a practical upper bound on the power law of $10^{2.6}$ km^2, and this is understood to be a physically meaningful upper bound reflecting restrictions on how many large glaciers can exist in glacierized regions of limited size, so we can fix $n = 10^{2.6}$ and do not need to worry about the convergence of these intervals as n increases. At the lower end of glacier areas, we do not have a physically meaningful cutoff for minimum glacier size m. We fix a lower limit of $10^{-2.0}$ km^2, because this is the smallest glacier size represented in RGIv5, but this is purely a limitation of the dataset, so in order to have physically plausible power laws, we should expect convergence in some of these integrals as m tends to zero. In equations (2) and (3), convergence is necessary as the total area and total volume of glaciers globally must be finite regardless of how small we make our minimum limit on glacier size, but equation (1) should not necessarily converge, because dropping the threshold for what we consider to be glaciers can plausibly add huge numbers of increasingly small ice masses. In essence, we can continue to add large numbers of increasingly small glaciers as long as they do not contribute a substantial overall area or volume. As $N(S)$ is proportional to S^b for the power-law exponent b, in order for equations (2) and (3) to converge as m tends to zero, we require, respectively:

$$b + 1 > -1 \tag{4}$$

$$b + 1.375 > -1 \tag{5}$$

Equation (5) is satisfied comfortably by every value of the exponent for all the power laws we generate, meaning that the total ice volume is at least theoretically consistent in every case. Equation (4) is satisfied comfortably for both the missing glacier power laws with and without Antarctic and Subantarctic glaciers, so the power-law explanation of 2015 glaciers is theoretically consistent. Both with and without Antarctic and Subantarctic glaciers, the upper-bound power laws based on 1901 glacier areas to derive disappeared-glacier contributions have error margins that straddle the $b = -2$ threshold for area convergence, and the corresponding power law for the lower bound is below but extremely close to the $b = -2$ threshold. This means there is uncertainty over whether the power law is too steep to be an accurate description of a possible 1901 glacier distribution if the minimum glacier size approaches zero. However, we do recognize that the inability of the model to account for the fact that separate modern glaciers may actually have been part of the same ice masses in the past when they were larger may 'bunch up' the distribution of smaller glaciers (and we note a slightly smaller exponent for the lower bound, where this effect is lessened). We therefore trust the estimate of the missing-glacier SLE mass-loss contribution more than the disappeared-glacier contribution, but we choose to include the figures as part of a consistent whole given that they originate from the same theoretical basis.

Code availability. The glacier model used[11] is available from the corresponding author on reasonable request. The remaining code consists of scripts for data processing that are not provided owing to their relative simplicity.

Data availability

The RGIv5 dataset used for glacier area distribution data are available from GLIMS at https://www.glims.org/RGI/randolph50.html with identifier doi:10.7265/N5-RGI-50. The updated glacier model output is available from the corresponding author upon reasonable request. The SGI is described in ref. [22] with identifier doi:10.1657/1938-4246-46.4.933, and data was available from the authors on reasonable request. The data generated for this paper is not provided owing to the difficulty of representing a collection of matrices indexed by glacier size class and year in a simple CSV file in a way that is easily readable, but the data is available from the corresponding author on reasonable request.

22. Fischer, M., Huss, M., Barboux, C. & Hoelzle, M. The new Swiss Glacier Inventory SGI2010: relevance of using high-resolution source data in areas dominated by very small glaciers. *Arct. Antarct. Alp. Res.* **46**, 933–945 (2014).
23. Bahr, D., Meier, M. & Peckham, S. The physical basis of glacier volume-area scaling. *J. Geophys. Res.* **102**, 20355–20362 (1997).
24. Bahr, D. Global distributions of glacier properties: a stochastic scaling paradigm. *Water Resour. Res.* **33**, 1669–1679 (1997).
25. Fischer, M., Huss, M. & Hoelzle, M. Surface elevation and mass changes of all Swiss glaciers 1980–2010. *Cryosphere* **9**, 525–540 (2015).

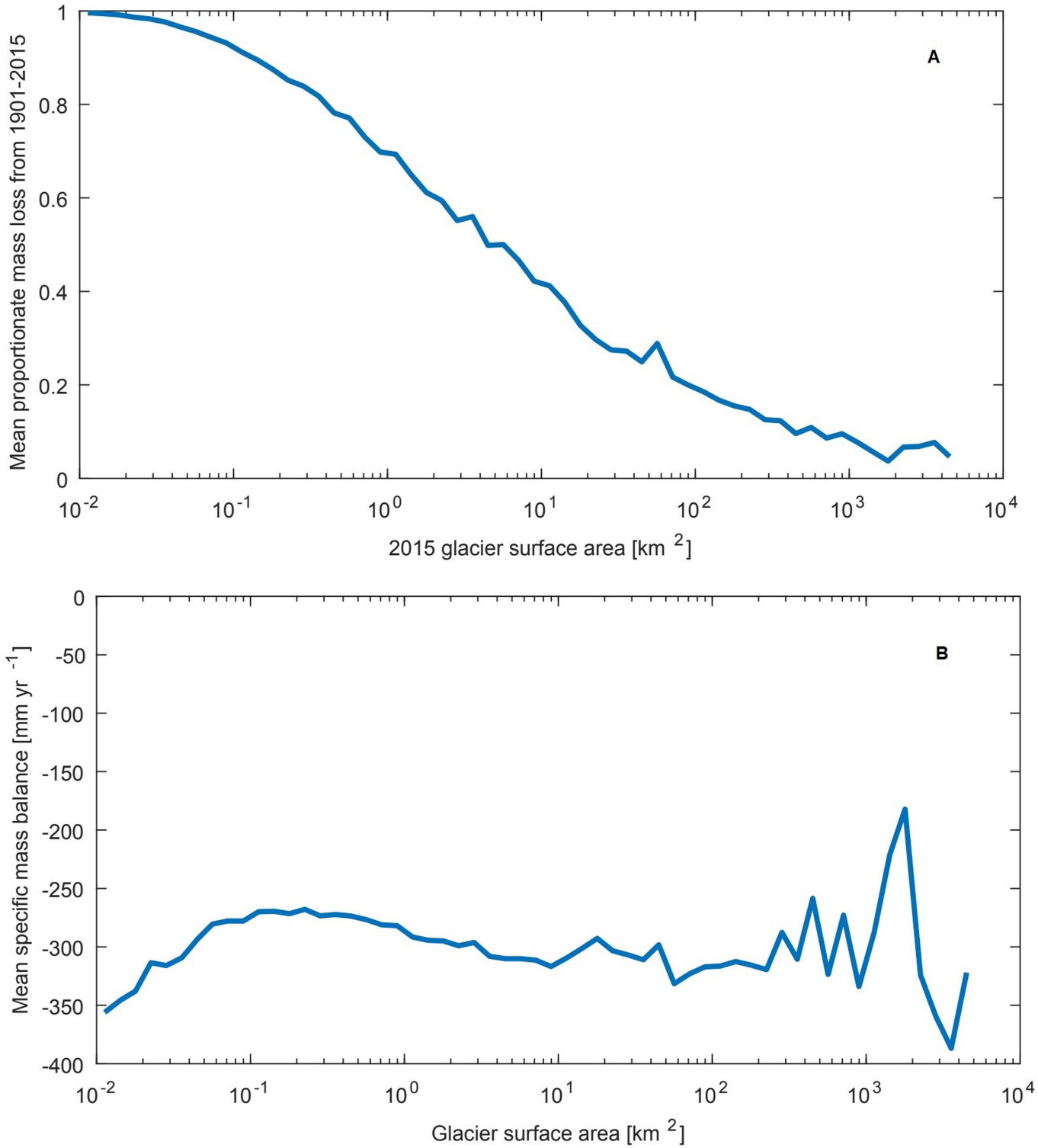

Extended Data Fig. 1 | RGIv5 glacier change statistics by size class. **a**, Mean specific glacier mass balance by glacier size class. The fact that this graph is relatively flat suggests that the differing mass balance between small glaciers and larger glaciers is not a driver for small glaciers (and by extension missing glaciers) contributing a large amount to SLE mass loss relative to their current ice mass. Glacier size does not strongly affect mean specific mass balance, and this weak dependence is also shown in observations from the literature[25]. **b**, Mean proportion of 1901 mass lost between 1901 and 2015 as a function of glacier size class. The smallest glaciers that exist in 2015 typically lost almost all of their 1901 mass, with the proportion dropping consistently as 2015 glacier size increases, up to the largest glaciers in 2015, which have seen an average of less than 10% of their mass disappear since 1901.

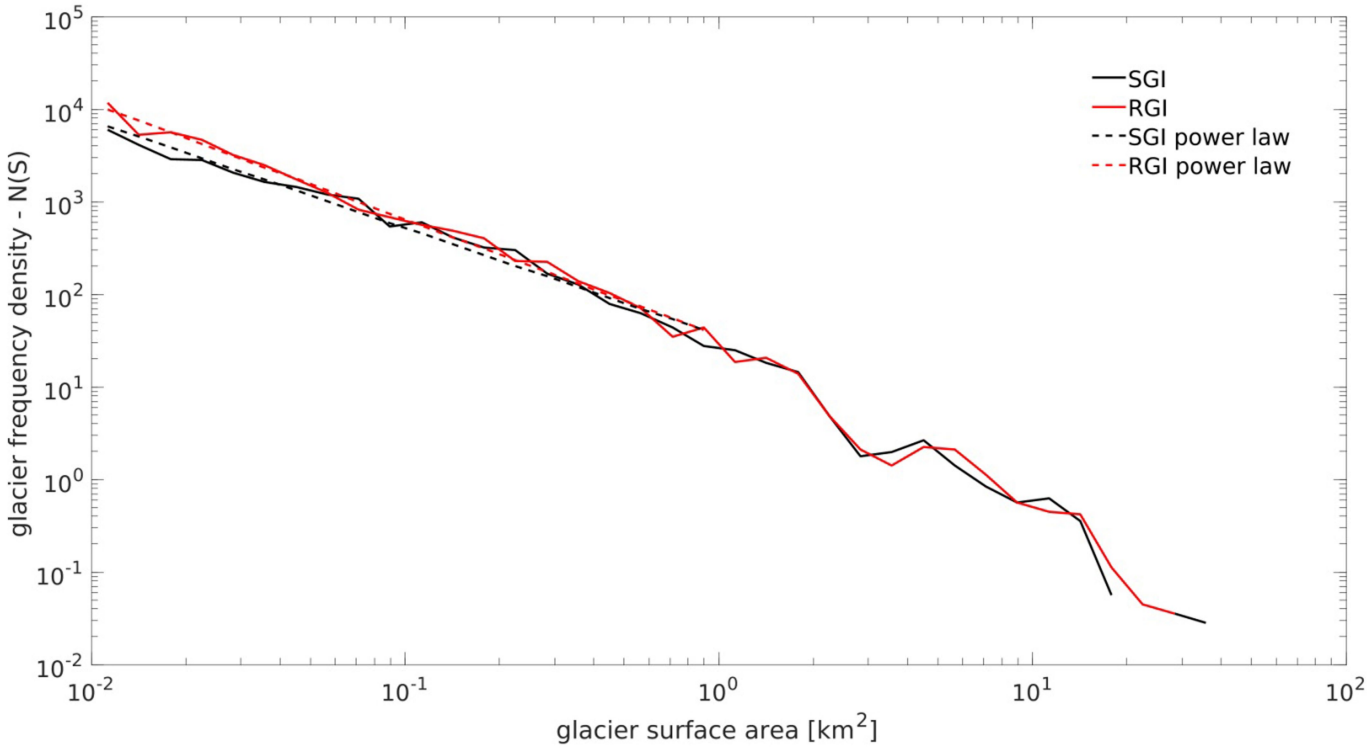

Extended Data Fig. 2 | Glacier distribution for Switzerland. We believe that in Switzerland, the RGIv5 (solid red) has a much better representation of small glaciers. The Swiss Glacier Inventory[22] (SGI) (solid black), which is based on high-resolution orthophotographs, and which is therefore believed to have better representation of small glaciers than is available globally, shows good agreement with the RGI. The power laws for the RGI and SGI (dashed red and dashed black respectively) are calculated for the 10^{-2} to 10^0 km^2 range, and show that a credible power law exists in this region down to the smallest glacier sizes, albeit with reduced exponents (1.26 and 1.16 respectively).

Extended Data Table 1 | Distribution of unmodelled glaciers

RGI Region	Percentage of glacierized area that cannot be modeled	Percentage of global small glacier area in this region
Alaska	0.2%	2.2%
Western Canada and US	0.7%	0.1%
Arctic Canada North	3.4%	8.5%
Arctic Canada South	0.7%	3.3%
Greenland Periphery	12.3%	43.1%
Iceland	0.0%	0.0%
Svalbard	6.2%	0.5%
Scandinavia	0.0%	0.0%
Russian Arctic	28.4%	1.4%
North Asia	4.7%	0.5%
Central Europe	2.7%	0.9%
Caucasus and Middle East	14.1%	2.4%
Central Asia	2.3%	19.3%
South Asia West	0.7%	3.6%
South Asia East	0.8%	1.6%
Low Latitudes	15.0%	4.8%
Southern Andes	0.8%	2.9%
New Zealand	0.9%	0.2%
Antarctic and Subantarctic	100.0%	4.7%

Each RGI region may contain glaciers for which the model fails. Antarctic and Subantarctic peripheral glaciers all fail owing to the absence of CRU data for the appropriate latitudes, while in other regions the iteration to find an initial 1901 glacier area fails in a minority of cases. The percentage of glacierized area in each region that cannot be modelled is shown alongside the percentage of global small-glacier area (all glaciers less than $10^{0.3}$ km^2 in size) in each region (which relates to how much the region affects the upscaling of small glaciers to account for uncharted glaciers). Notably, the Greenland Periphery region contains a disproportionately large amount of the world's total small-glacier area, while the Antarctic and Subantarctic region contains relatively little. At present, we are unable to determine whether this is primarily due to differing regional distributions (for example, Antarctica has more large glaciers but fewer small glaciers than Greenland) or differing data quality.